Drosophila melanogaster Cad99C, the orthologue of human Usher cadherin PCDH15, regulates the length of microvilli

Cecilia D'Alterio, Dao D.D. Tran, Maggie W.Y. Au Yeung, Michael S.H. Hwang, Michelle A. Li, Claudia J. Arana, Vikram K. Mulligan, Mary Kubesh, Praveer Sharma, Maretta Chase, Ulrich Tepass, and Dorothea Godt

Department of Zoology, University of Toronto, Toronto, Ontario, Canada, M5S 3G5

Actin-based protrusions can form prominent structures on the apical surface of epithelial cells, such as microvilli. Several cytoplasmic factors have been identified that control the dynamics of actin filaments in microvilli. However, it remains unclear whether the plasma membrane participates actively in microvillus formation. In this paper, we analyze the function of *Drosophila melanogaster* cadherin Cad99C in the microvilli of ovarian follicle cells. *Cad99C* contributes to eggshell formation and female fertility and is expressed in follicle cells, which produce the eggshells. Cad99C specifically localizes to apical microvilli. Loss of Cad99C function results in shortened and disorganized microvilli, whereas overexpression of Cad99C leads to a dramatic increase of microvillus length. Cad99C that lacks most of the cytoplasmic domain, including potential PDZ domain–binding sites, still promotes excessive microvillus outgrowth, suggesting that the amount of the extracellular domain determines microvillus length. This study reveals Cad99C as a critical regulator of microvillus length, the first example of a transmembrane protein that is involved in this process.

Introduction

Microvilli are fingerlike protrusions on the apical surface of epithelial cells, where they can form a dense brush border. Microvilli are also used by several sensory cells as a basic module to form specialized structures that engage in the transduction of light and mechanosensory stimuli. Stereocilia of vertebrate inner ear hair cells are a prominent example (for review see Müller and Littlewood-Evans, 2001). The core of a microvillus consists of a bundle of cross-linked parallel actin filaments, which have their barbed (+) ends inserted at the microvillus tip and their pointed (−) ends anchored in a terminal web of actin filaments (for reviews see Bartles, 2000; DeRosier and Tilney, 2000; Lin et al., 2005). The actin filament bundle undergoes constant turnover through treadmilling (Rzadzinska et al., 2004). Growth of microfilaments at barbed ends is thought to push the membrane envelope forward, lengthening the protrusion (for review see Lin et al., 2005).

Among the molecules that serve a critical function in the formation and regulation of microvillus growth are several F-actin cross-linking proteins, including villin, epsin, fimbrin, and fascin (for reviews see DeRosier and Tilney, 2000; Müller and Littlewood-Evans, 2001; Lin et al., 2005). Epsin can induce microvillus elongation in vitro probably by affecting the actin treadmilling process (Loomis et al., 2003; Sekerkova et al., 2004), and epsin mutant *deaf jerker* mice have shortened hair cell stereocilia (Zheng et al., 2000). Additional actin-binding factors that control microvillus size colocalize with the tip complex, which is thought to nucleate the microfilament bundle and to regulate actin polymerization at barbed ends. They comprise myosin XVa and its binding partner whirlin, which promote concentration-dependent elongation of hair cell stereocilia (Belyantseva et al., 2003, 2005; Mburu et al., 2003; for review see Lin et al., 2005). EPS-8, another actin-binding protein located at a microvillus tip, regulates microvillus length through its barbed-end capping function in the intestine of *Caenorhabditis elegans* (Croce et al., 2004). In the early *Drosophila melanogaster* embryo, absence of the Abelson kinase causes abnormally long microvilli, which correlates with an ectopic accumulation of F-actin and its growth promoting factor Enabled in the apical cell cortex (Grevengoed et al., 2003).

Observations like these suggested that microfilaments and their binding factors may be sufficient for microvillus for-

Correspondence to Dorothea Godt: dgodt@zoo.utoronto.ca

Abbreviations used in this paper: CD, cadherin domain; CDH23, cadherin 23; dsRNA, double-stranded RNA; PCDH15, protocadherin 15; RNAi, RNA interference; USH1, usher syndrome type 1; VM, vitelline membrane.

The online version of this article contains supplemental material.

The Journal of Cell Biology, Vol. 171, No. 3, November 7, 2005 549–558
http://www.jcb.org/cgi/doi/10.1083/jcb.200507072

mation and elongation and that the plasma membrane may serve only as an anchor for the core bundle (for review see Borisy and Svitkina, 2000). That coupling to the plasma membrane is important is suggested by the finding that ezrin, an ERM (ezrin–radixin–Moesin) protein that likely forms a link between actin filaments and the plasma membrane, induces microvilli in cell culture (Gautreau et al., 2000). Deficiency of ezrin, which appears to organize the terminal web of microvilli, causes shortened, irregular intestinal microvilli in mice (Saotome et al., 2004). Similarly, the terminal web–associated ERM protein Moesin in *D. melanogaster* is required for normal organization of microvilli in rhabdomeres, and an excessive formation of irregular microvilli results from expressing constitutively active Moesin (Karagiosis and Ready, 2004). However, there has been no evidence so far that would implicate specific integral membrane proteins as regulators of microvillus growth.

Some proteins that have received considerable attention in recent years as important organizers of hair cell stereocilia are protocadherin 15 (PCDH15), cadherin 23 (CDH23), myosin VIIa, harmonin, and SANS. Mutations in these genes are responsible for Usher syndrome type 1 (USH1), a genetic disorder that combines congenital deafness, vestibular dysfunction, and retinitis pigmentosa in humans (for review see Petit, 2001; Ahmed et al., 2003b; Frolenkov et al., 2004). The phenotype of mice mutant for any USH1 gene is characterized by splayed and disorganized stereocilia and consequently it was proposed that the two USH1 cadherins may contribute to the links that visibly connect neighboring stereocilia (for review see Frolenkov et al., 2004). For CDH23, this model is supported by the observations that it colocalizes with lateral and tip links, is needed for tip link integrity, and can mediate homophilic adhesion (Siemens et al., 2004; Söllner et al., 2004; Michel et al., 2005). The molecular function of PCDH15, however, has not been elucidated. In this paper, we report that Cad99C, the fly orthologue of PCDH15, is a component of microvilli and show by loss- and gain-of-function analysis that Cad99C promotes microvillus elongation in a concentration-dependent manner. Our data also suggest that Cad99C acts through a mechanism that does not involve adhesion between microvilli.

Results

Cad99C is expressed in follicle cells during oogenesis

To identify novel regulators of cell and tissue morphogenesis, we studied the expression patterns of uncharacterized members of the cadherin gene superfamily (for review see Tepass et al., 2000; Hill et al., 2001) during *D. melanogaster* oogenesis, when follicle cells undergo a series of well-described morphogenetic movements (for review see Horne-Badovinac and Bilder, 2005). *Cad99C*, a cadherin gene that we named after its chromosomal map position, is transcribed in cells of the follicular epithelium, but not in the germline cyst (Fig. 1, A–F). Changes in the *Cad99C* expression level largely coincide with morphogenetically active phases of follicle cells. *Cad99C* mRNA was found in anterior and posterior follicle cells at stages 2–5 but was restricted to posterior follicle cells at late stage 6. Follicle cells that move over the oocyte at stage 9 and form a columnar epithelium at stage 10a expressed very high levels of *Cad99C* transcript. By stage 10b, high levels of expression were retained only in centripetal follicle cells that migrate inward to envelope the oocyte anteriorly. Expression levels peaked again in all follicle cells when they flattened to accommodate the growth of the oocyte. During late oogenesis, some follicle cells form tubelike structures—the micropyle and dorsal appendages—which is a process accompanied by a local increase of *Cad99C* expression. This dynamic expression profile suggested that *Cad99C* makes important contributions to follicle cell development. Consistent with its mRNA distribution, Cad99C protein (Fig. 1, G and H) was first seen during stages 2–5 of oogenesis in anterior and posterior terminal follicle cells. Beginning with stage 6, Cad99C was only detected in follicle cells that are in contact with the oocyte, a distribution that persists for the rest of oogenesis. At all stages, Cad99C was located on the apical plasma membrane of follicle cells, which faces the oocyte.

Cad99C is the orthologue of mammalian PCDH15

Gene annotation and cDNA analysis predict that *Cad99C* (*CG310034*; Celniker et al., 2002) encodes a single-pass transmembrane protein with 11 cadherin domains (CDs; Fig. 2 B).

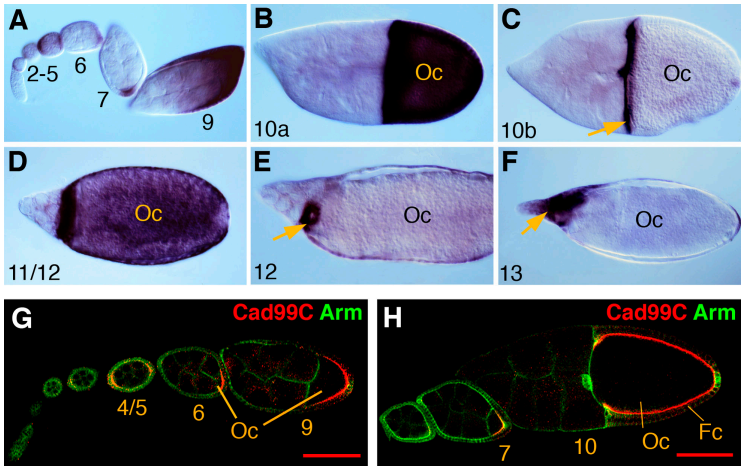

Figure 1. **Expression of Cad99C during oogenesis.** (A–F) Distribution of *Cad99C* mRNA in egg chambers at different stages of oogenesis. Arrows point to centripetal follicle cells in C, micropyle-forming follicle cells in E, and dorsal appendages in F. (G and H) Cad99C protein (red) is found on the apical surface of follicle cells (Fc) and from stage 6 onward is only seen in follicle cells that contact the oocyte (Oc). Armadillo (Arm; green) labels the membranes of germline and follicle cells. Numbers indicate stages of oogenesis. Bars, 100 μm.

The cytoplasmic tail of Cad99C is asparagine rich and contains the motif SEVETTTEL at the COOH terminus, in which the underlined residues fit the consensus S/T–X–L/V of class 1 PDZ domain–binding sites (Sheng and Sala, 2001). Cad99C is conserved in *Anopheles gambiae* and *Apis mellifora*, showing 62 and 52% identity in the extracellular region and 44 and 32% in the cytoplasmic tail, respectively. The closest relative in humans is PCDH15. Cad99C and PCDH15 have very similar protein architectures (Fig. 2 B). They show 30% identity across the 11 extracellular CDs (expect value is e^{-121}; Fig. S1, available at http://www.jcb.org/cgi/content/full/jcb.200507072/DC1). In comparison, there is 24% identity between the 11 CDs of Cad99C and the first 11 CDs or next 11 CDs of human fat3 (e^{-57} and $3e^{-63}$, respectively), a cadherin that gives the second best score in a Blast search. PCDH15 also contains a COOH-terminal PDZ-binding site (SQSTSL; Adato et al., 2005); otherwise, no significant similarity was identified in the cytoplasmic tail. It is noteworthy that the cytoplasmic tail is substantially diverged even between mouse and human PCDH15, showing only 57% identity, in contrast to 94% identity in the extracellular portion.

In classic cadherins, binding of Ca^{2+} leads to dimerization and rigidification of CDs and is essential for the function of cadherins as adhesion molecules. Ca^{2+} associates with the linker region between CDs, requiring specific amino acid residues from both neighboring CDs (for review see Tepass et al., 2000; Patel et al., 2003; Koch et al., 2004). Interestingly, Cad99C and PCDH15 lack consensus sites for Ca^{2+}-binding at conserved positions, between CDs 5/6 and 9/10, which are among the best-conserved CDs (36–39% identity; Fig. S1). This suggests that the extracellular region of Cad99C/PCDH15 is composed of two extended rodlike parts (CDs 1–5 and 6–9) connected by a potentially flexible hinge. CD 9 is followed by another hinge region that links to a pair of Ca^{2+}-associated CDs (Fig. 1 B). The similarities in protein structure strongly suggest that Cad99C is the orthologue of PCDH15.

Cad99C loss-of-function mutations cause female sterility

The chromosomal interval 99C is poorly characterized, and available deletions are haplolethal. To determine the function of *Cad99C*, we generated mutations by imprecise excision of two *P* elements. *GE21034* is inserted upstream of the sequences that have been reported to represent exon 1 of *Cad99C,* and *GE23478* is located in intron 1 (Fig. 2 A; Schlichting et al., 2005; http://genexel.com/eng/htm/genisys.htm). Both *P* element insertions were homozygous viable. However, whereas *GE21034* appeared fully fertile, *GE23478* females showed reduced fertility that was fully restored by excision of *GE23478*, indicating that the *P* element insertion was responsible for this defect. Several excision lines were female sterile (but male fertile; see next section) and had subtle bristle and eye defects (unpublished data). These lines failed to complement each other, and molecular analysis showed that they represent genomic deletions within *Cad99C* (Fig. 2 A). In $Cad99C^{21\text{-}6}$, we detected a small deletion removing exon 1, which is noncoding. The largest deletions are $Cad99C^{21\text{-}8}$ and $Cad99C^{21\text{-}5}$, with the latter removing most of the coding sequence for the extracellular domain (CDs 1–8 and part of CD 9).

Cad99C antibodies, raised against a portion of the extracellular (CDs 10 and 11) and cytoplasmic domains (Fig. 2 B), were used to probe Cad99C expression in ovaries of wild-type and homozygous *Cad99C* mutant females, respectively. Immunoblots identified three protein bands in wild type that were absent in mutants that lack exon 1—$Cad99C^{21\text{-}5}$, $Cad99C^{21\text{-}6}$, and $Cad99C^{21\text{-}8}$ (Fig. 2 C). Cad99C protein was also strongly reduced in ovaries that expressed *Cad99C* double-stranded RNA (dsRNA) causing RNA interference (RNAi; Fig. 2 C). The major band corresponds to ~217 kD, which is 30 kD larger than the predicted size of Cad99C, a difference that is partly attributable to N-linked glycosylation (unpublished data). Two weak additional bands (195 and 172 kD) varied in intensity between preparations (inverse proportional to

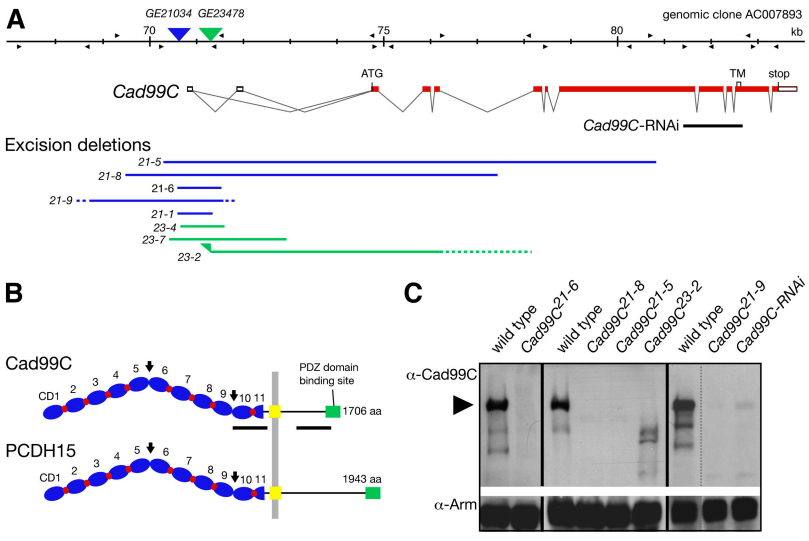

Figure 2. **Molecular analysis of *Cad99C*.** (A) Genomic map of the *Cad99C* transcription unit. The ORF is in red. Deletions derived from *P* element insert *GE21034* are shown in blue and those from *GE23478* in green. A dotted line indicates the uncertainty interval of a breakpoint. Triangles indicate primers used to map the deletion breakpoints. A black bar indicates the region used for RNAi. TM, transmembrane domain. (B) Cad99C and PCDH15 have a similar protein structure characterized by 11 CDs (blue), a single transmembrane domain (yellow), and a PDZ domain–binding site at the COOH terminus (green). Potential Ca^{2+}-binding sites between CDs are shown in red. Arrows point to linker regions that presumably cannot bind Ca^{2+}. Black bars indicate regions used for generation of antibodies. (C) Immunoblot analysis of Cad99C expression in ovaries. Cad99C antibodies (extracellular epitope; B) reveal a major protein of ~217 KD (arrowhead) in wild type that is not detected in *Cad99C* mutants and severely reduced after *Cad99C* RNAi. The two smaller proteins (195 and 172 kD) found in wild type but not in mutant ovaries may represent degraded or otherwise modified Cad99C products. Only the $Cad99C^{23\text{-}2}$ allele, which still contains exon 1 in contrast to other alleles (A), produces detectable amounts of protein, albeit of reduced size.

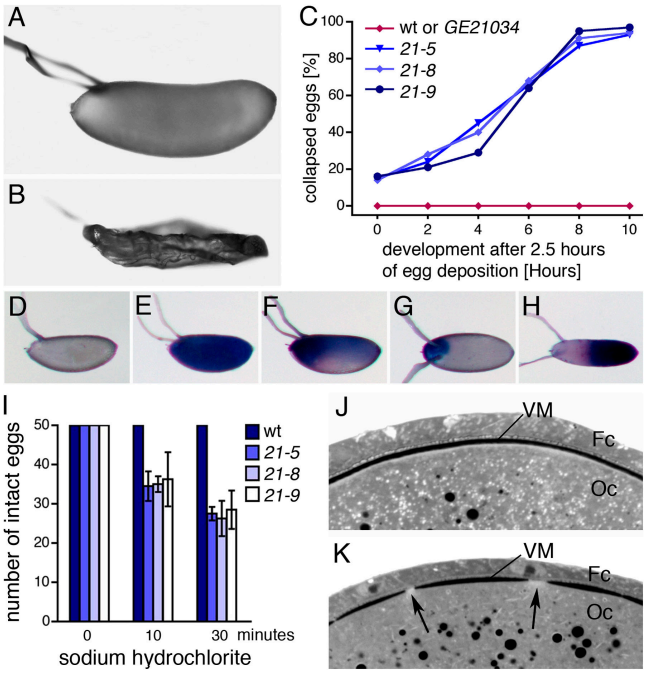

Figure 3. **Eggs derived from *Cad99C* mutant females have a defective VM.** (A) A wild-type *D. melanogaster* egg. (B) A collapsed egg from a *Cad99C*$^{21\text{-}5}$ mutant female. (C) Eggs from *Cad99C* mutant mothers dehydrated over time. By mid-embryogenesis >90% of the eggs were collapsed. Eggs from the *P* insertion line *GE21034*, the progenitor of the *Cad99C* mutant lines, did not collapse. Numbers of examined eggs: wild type (wt), $n = 468$; *GE21034*, $n = 367$; *Cad99C*$^{21\text{-}5}$, $n = 325$; *Cad99C*$^{21\text{-}8}$, $n = 375$; *Cad99C*$^{21\text{-}9}$, $n = 245$. (D) Trypan blue did not penetrate wild-type eggs but stained to a variable degree eggs from *Cad99C*$^{21\text{-}9}$ (E–G) and *Cad99C*$^{21\text{-}5}$ (H) mutant mothers. In most eggs, the anterior region was stained strongest. (I) In contrast to normal eggs, 50% of the eggs from *Cad99C* mutants had disintegrated in sodium hydrochlorite after 30 min. The histogram shows mean values and SDs based on four experiments. (J and K) Histological sections of stage 11 egg chambers show that the VM is continuous in wild type (J) but has gaps in a *Cad99C*$^{21\text{-}8}$ mutant follicle (K, arrows). Oc, oocyte; Fc, follicle cells.

the intensity of the major band) and may represent degraded or otherwise modified Cad99C protein. Together, our results suggest that we isolated null mutations for *Cad99C* and that this gene is not essential for viability but required for female fertility.

Eggshell formation is compromised in *Cad99C* mutants

The female-sterile phenotype of *Cad99C* mutants is caused by defects in eggshell formation as revealed by the following analysis. *Cad99C*$^{21\text{-}5}$, *Cad99C*$^{21\text{-}8}$, or *Cad99C*$^{21\text{-}9}$ mutant females laid ~50% fewer eggs than wild-type females, and <2% of those eggs ($n > 300$ per genotype) produced larvae. These larvae developed into flies that only displayed defects if they were homozygous mutants, and those defects are the same as in homozygous mutants derived from heterozygous mothers, suggesting that maternal loss of *Cad99C* has no effect on postembryonic development. The majority of eggs from *Cad99C* mutant females collapsed soon after deposition (Fig. 3, A–C), and even noncollapsed eggs were penetrable to the vital dyes neutral red and trypan blue (Fig. 3, D–H), which do not stain wild-type eggs (Mahowald, 1972; LeMosy and Hashimoto, 2000). These defects suggested that eggshells, which normally restrict permeability and prevent desiccation (Limbourg and Zalokar, 1973; Mahowald and Kambysellis, 1980), are compromised. Eggs from mutant females were also highly intolerant to sodium hydrochlorite. Hydrochlorite treatment of wild-type eggs removes the outer eggshell, the chorion, but leaves the inner eggshell, the vitelline membrane (VM), intact (Limbourg and Zalokar, 1973). Disintegration of eggs from *Cad99C* mutant females in hydrochlorite suggests that the VM is not functional (Fig. 3 I). The VM normally forms a continuous layer of homogeneous thickness in late follicles (Mahowald and Kambysellis, 1980), whereas the VM of *Cad99C* mutant follicles varied in thickness and contained numerous holes (Fig. 3, J and K). These holes are likely the cause for the observed desiccation of eggs. The variability in eggshell defects may explain why mutant females are not fully sterile, allowing a few embryos to develop. The importance of *Cad99C* for proper eggshell formation is consistent with its expression in follicle cells that secrete the eggshell material.

Cad99C is a component of follicle cell microvilli

To address the function of Cad99C in the follicular epithelium, we first examined the subcellular localization of this cadherin and found that it is confined to the apical microvillus brush border. Cad99C is located apical to DE-cadherin (Fig. 4 A) and DPatj (Fig. 4 B), which mark the adherens junctions and apical cell cortex, respectively (Oda et al., 1994; Tanentzapf et al., 2000). In contrast to DE-cadherin, Cad99C is not seen at the apicolateral and lateral plasma membrane, where follicle cells are in contact with one another. Cad99C shows a spiky pattern in a side view (Fig. 4, A and D) and a carpetlike pattern in a front view of the apical cell surface (Fig. 4 E), which is consistent with a localization to microvilli. Several observations support that Cad99C is specific for follicle cell microvilli and not found in oocyte microvilli, with which they make contact. First, *Cad99C* expression was not detected in the germline (Fig. 1, A–F). Second, the pattern of Cad99C-positive microvilli reflects the honeycomb pattern of follicle cells (Fig. 4 E), whereas oocyte microvilli form a continuous lawn (Mahowald and Kambysellis, 1980). Third, Cad99C does not overlap with Yolkless, a marker that labels the oocyte cortex (Fig. 4 C; Schönbaum et al., 2000) but colocalizes with a marker specifically expressed in follicle cells (CD8-GFP; Fig. 4 F). We infer that Cad99C does not mediate homophilic adhesion between follicle cells or between microvilli of follicle cells and those of the oocyte.

As a marker for follicle cell microvilli, Cad99C revealed that the length of these apical protrusions increases from stage 7 to late stage 10a (Fig. 4, G, H, and K), when they reach their maximum extent of 2–3 μm. At stage 10a, longer microvilli are found in the center and shorter ones in the periphery of the apical follicle cell surface (Fig. 4 D). After stage 10, microvilli regress, but short microvilli remain until the end of oogenesis (Fig. 4, I, J, and L). Concurrent with the development of the microvillus brush border, follicle cells secrete VM material into the extracellular space between microvilli, producing so-

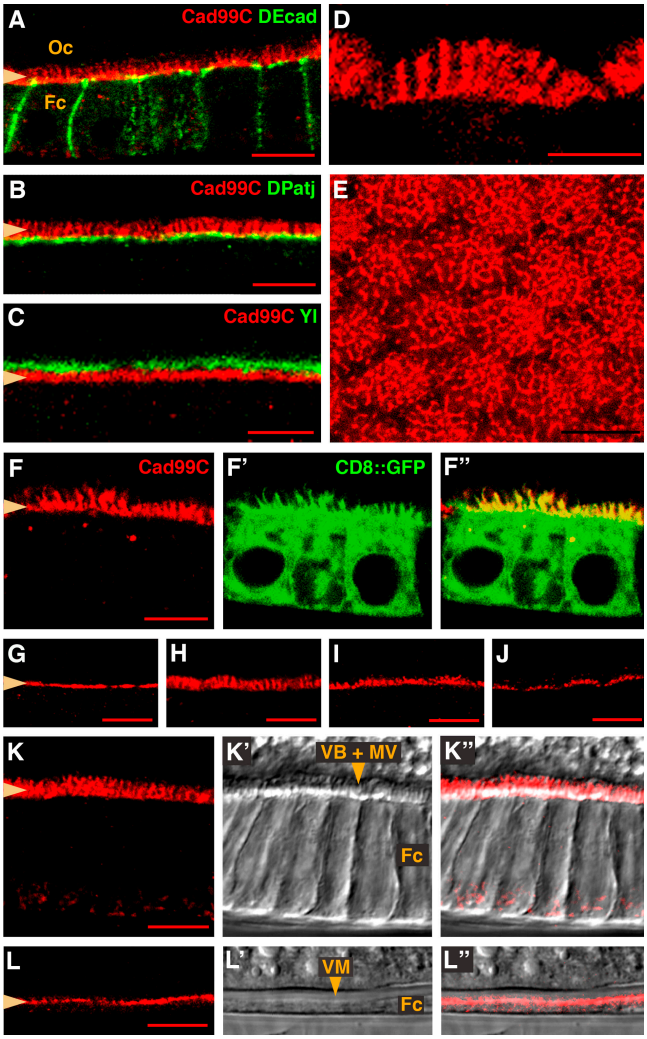

Figure 4. **Cad99C localizes to the apical microvilli of follicle cells.** Cad99C is always red. Confocal images of the follicular epithelium are from egg chambers at stage 10 in A–F or the indicated stage in G–L. Nomarski images are shown in panels marked with ' or ". (A and B) Cad99C is located apical to the adherens junction marker DE-cadherin (DEcad) and the apical cortex marker DPatj of follicle cells. Bars, 10 μm. (C) Cad99C distribution does not overlap with the oocyte cortex marker Yolkless (Yl). Bar, 10 μm. (D) Apical microvilli of follicle cells can be seen individually at stage 10a. Bar, 5 μm. (E) The pattern of Cad99C positive microvilli reflects the hexagonal array of follicle cells in a top view. Bar, 10 μm. (F–F") Cad99C colocalizes with the apical CD8::GPF staining in follicle cells. CD8::GFP, which is expressed only in follicle cells using *da-Gal4* as a driver, outlines all plasma membrane structures of follicle cells, including the apical microvillus brush border. Bar, 10 μm. (G–J) Cad99C staining reflects the dynamic changes in microvillus length: a strong growth from stage 9 (G) to late 10a (H), and a progressive shortening from stage 10b (I) to stage 11 (J). Bars, 10 μm. (K–K") The microvillus brush border of follicle cells forms a distinct band in a Nomarski image (K'). The stripe pattern of this band reflects the alternate arrangement of microvilli and vitelline bodies at stage 10 of oogenesis. Bar, 10 μm. (L–L") At stage 12, follicle cell microvilli are much shorter than at stage 10 and the vitelline bodies have fused into a layer, the VM. Bar, 10 μm. The apical surface of follicle cells, which faces the overlying oocyte, is marked by an arrowhead in A–C, F, G, K, and L. Oc, oocyte; Fc, follicle cells; MV, microvilli; VB, vitelline bodies.

called vitelline bodies, which correspond in height to the microvilli (Fig. 4 K') and subsequently fuse into a continuous VM layer above the microvilli (Fig. 4 L'; Mahowald and Kambysellis, 1980). The extracellular space seen between individual microvilli at the light-microscopic level suggests a separation of >400 nm (Fig. 4, A and D). With a predicted length of 50 nm for the Cad99C extracellular region, a Cad99C trans-dimer would not be able to bridge such a gap. It therefore appears unlikely that Cad99C promotes homophilic adhesion between adjacent microvilli along their entire length, although spotlike sites of adhesion cannot be excluded.

Cad99C mutations affect length, shape, and arrangement of follicle cell microvilli

To analyze microvillus formation in the absence of Cad99C, we examined the distribution of F-actin and the membrane marker CD8-GFP. In wild type, F-actin is seen in microvilli of follicle cells and is enriched in the cortex of follicle cells and oocyte (Fig. 5 A). In *Cad99C* mutant follicles, F-actin staining is strongly reduced in the space between follicle cells and oocyte, suggesting defective microvilli (Fig. 5 B). CD8::GFP labeling revealed a regular microvillus brush border in wild-type follicle cells (Fig. 5, C' and F), whereas *Cad99C* mutant follicle cells displayed a range of defects of microvilli (Fig. 5, D, E, and G). In all mutant follicles, microvilli appeared substantially shorter than in wild type (Fig. 5, D and E). In many cases, apical protrusions appeared reduced in number, and they formed an irregular spiky pattern, suggesting that microvilli are abnormally shaped and may be clumped. In other cases, no obvious protrusions were detected or only few microvilli with an abnormal, wavy shape protruded from the apical surface (Fig. 5, E and G). Expression of *Cad99C* dsRNA caused the same type of microvilli defects as *Cad99C* mutations (Fig. 5 H). The persistent strong CD8::GFP labeling of the apical membrane domain even in cases where no protrusions were detected indicates that a substantial amount of membrane material is retained apically. These findings argue against a complete loss of microvilli and suggest that microvilli are strongly shortened and may also be collapsed against the apical cell surface. Together, these data show that Cad99C is essential to form microvilli of normal length and organization in follicle cells.

Egg chambers of *Cad99C* mutants have vitelline bodies that are irregular in size, shape, and distribution (Fig. 5, K and L). This suggests that the defective microvilli may cause an abnormal secretion or distribution of extracellular proteins. To address this problem, we examined the distribution of Nudel, a secreted protein that is involved in proper formation of eggshells and the dorsal–ventral axis (LeMosy et al., 1998; LeMosy and Hashimoto, 2000). No difference was noted between *Cad99C* mutant and wild-type follicles in the distribution or amounts of Nudel, which was deposited to its proper location between oocyte membrane and VM material (Fig. 5, I and J). This finding argues against a general defect in protein secretion in *Cad99C* mutants.

Overexpression of Cad99C increases microvillus length

To determine whether Cad99C is a limiting factor for microvillus outgrowth, we overexpressed full-length Cad99C (Cad99C-FL; Fig. 6 H) in follicle cells. Cad99C-FL expression induced a striking increase in the length of apical microvilli (Fig. 6 A). These long cellular protrusions, which sometimes exceeded the

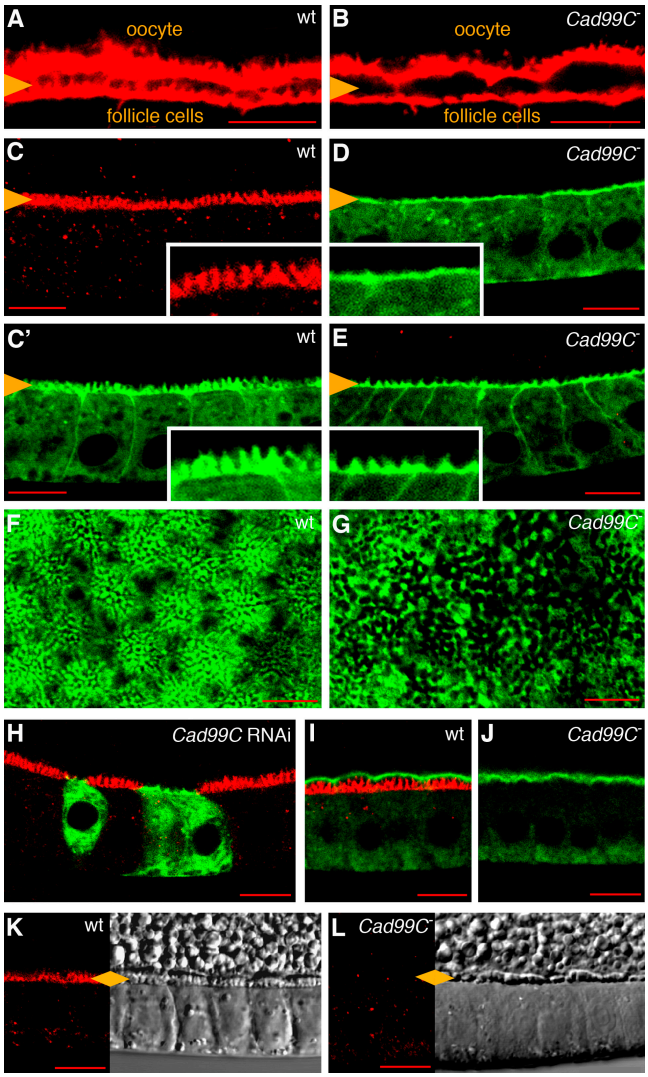

Figure 5. **Loss of Cad99C causes defects in the microvillus brush border of follicle cells.** All panels show a confocal section of the follicular epithelium of late stage 10a egg chambers. The oocyte is up. (A) In wild type, sandwiched between the F-actin–rich cortices of oocyte and follicle cells, are the actin filament bundles of follicle cell microvilli (arrowhead). (B) F-actin–rich protrusions on the apical surface of follicle cells are largely missing in a *Cad99C*$^{21\text{-}8}$ mutant egg chamber. (C and C') Microvilli in phenotypically wild-type follicles (*Cad99C*$^{21\text{-}8}$/+) are visualized by Cad99C (C, red) or CD8::GFP (C', green) and shown at higher magnification in insets. Expression of *UAS-CD8::GFP* was induced by *Act5c>CD2>Gal4*. (D and E) Examples of *Cad99C*$^{21\text{-}8/21\text{-}6}$ mutant follicles stained with CD8::GFP (green), showing that microvilli, which are displayed at higher magnification in insets, are strongly reduced in size and irregular in shape and arrangement. (F) Top view showing regular microvilli tufts on the apical surface of normal (*Cad99C*$^{21\text{-}8}$/+) follicle cells stained with CD8::GFP. (G) In contrast, the apical surface of *Cad99C*$^{21\text{-}8/21\text{-}6}$ mutant follicle cells shows an irregular distribution of microvilli. (H) *Cad99C* dsRNA was coexpressed with CD8::GFP (green) in follicle cell clones. These cells do not express Cad99C (red) and show strongly reduced microvilli compared with neighboring Cad99C expressing wild-type cells. In wild type (I) and *Cad99C*$^{21\text{-}8}$ mutants (J), Nudel protein (green) is secreted by follicle cells and located in the extracellular space between follicle cells and oocyte. Wild-type microvilli contain Cad99C (red). (K and L) The Nomarski image reveals a regular striped band of microvilli and vitelline bodies in wild type (K) but shows a disrupted irregular band in a *Cad99C*$^{21\text{-}8}$ mutant (L). Accompanying confocal images show the presence (K) and absence (L) of Cad99C (red). An arrowhead points to the microvillus brush border in A–E, K, and L. wt, wild type; *Cad99C*$^{-}$, *Cad99C* mutant. Bars, 10 μm.

apical–basal length of the follicle cells, projected into the narrow space between follicle cells and oocyte (Fig. 6, A, E, and F). Very long extensions showed small knoblike dilatations. Interestingly, the vitelline bodies deposited between the overlong microvilli also appeared enlarged (Fig. 6 A'). Furthermore, expression of Cad99C-FL rescued microvillus formation in a *Cad99C* mutant background (Fig. 6 B). To investigate the importance of cytoplasmic interactions for Cad99C function, we expressed a transgenic protein (Cad99CΔcyt::GFP; Fig. 6 H) in which GFP replaces a large portion of the cytoplasmic tail, including the PDZ-binding sites. Strikingly, Cad99CΔcyt::GFP induced abnormally tall microvilli that fanned out from the apical surface and enlarged vitelline bodies similar to Cad99C-FL. This effect was observed in a wild-type (Fig. 6 C) and in a *Cad99C* mutant background (Fig. 6, D and G). These data suggest that Cad99C levels determine the length of microvilli and show that the majority of the cytoplasmic domain (256 out of 287 amino acids) can be deleted without affecting the potential of Cad99C to promote microvillus outgrowth.

Discussion

Cad99C controls microvillus length by a concentration-dependent mechanism

Our study shows that the loss of Cad99C results in shorter microvilli and overexpression in longer microvilli than in wild type (Fig. 7, A and B), indicating that the concentration of Cad99C is positively correlated with the length of microvilli in follicle cells. Interestingly, modifications in the *Cad99C* mRNA expression level during oogenesis appear to be good indicators for changes in microvilli. During mid-oogenesis, prominent expression of *Cad99C* is seen in follicle cells that show forming and growing apical microvilli (Fig. 1, A, G, and H; Fig. 4 G; and not depicted), and *Cad99C* expression culminates when microvilli reach their maximum extension (Fig. 1 B and Fig. 4 H). The following drop of mRNA levels in most follicle cells coincides with a regression of microvillus size (Fig. 1 C and Fig. 4, I and J), whereas centripetal cells express *Cad99C* strongly (Fig. 1 C), consistent with the delayed formation of a microvillus brush border by these follicle cells (Mahowald and Kambysellis, 1980; unpublished data). We therefore propose that transcriptionally regulated changes in the concentration of Cad99C are critically involved in the dynamic remodeling of follicle cell microvilli.

The loss of Cad99C, which results in microvilli defects, also leads to defects in eggshell formation, suggesting that normal microvilli have an important function in eggshell development. Interestingly, the dynamic regulation of *Cad99C* expression correlates well temporally and spatially with described phases of eggshell secretion (for review see Spradling, 1993) and with morphogenetic movements of follicle cells, which raises the question of how these processes are interrelated. Follicle cells undergo multiple morphogenetic movements to reach positions from which they secrete eggshell material either while the movement is being completed or immediately afterwards (for review see Spradling, 1993). Therefore, the striking correlation between the Cad99C expression profile and morphogenetic movements likely re-

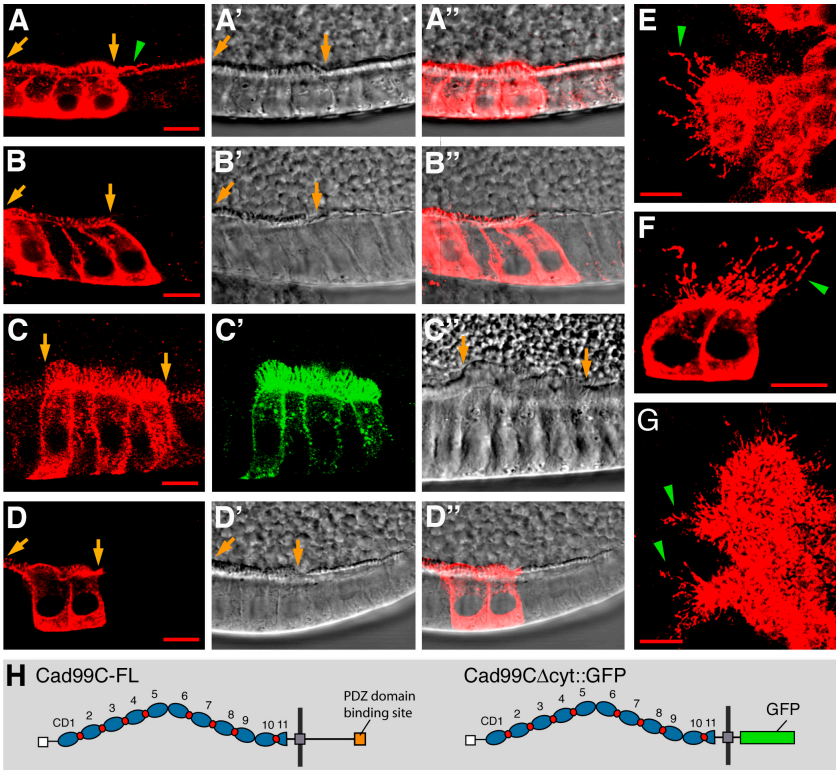

Figure 6. **Overexpression of Cad99C increases microvillus length.** Transgenic proteins Cad99C-FL and Cad99CΔcyt::GFP were expressed in cell clones in the follicular epithelium using *Act5c>CD2>Gal4*. Cad99C is in red. (A–A″) Cells that express Cad99C-FL produced abnormally tall microvilli. A green arrowhead marks long microvilli projecting into wild-type territory. (B–B″) Expression of Cad99C-FL rescued the microvillus phenotype of a $Cad99C^{21\text{-}5/21\text{-}6}$ mutant. (C–C″) Expression of Cad99CΔcyt::GFP induced lengthening of microvilli as seen with Cad99C (C, red) or GFP (C′, green). (D–D″) Cad99CΔcyt::GFP expression rescued the microvilli in a $Cad99C^{21\text{-}5/21\text{-}6}$ mutant follicle. Cad99C-FL (E and F) and Cad99CΔcyt::GFP (G) induce giant microvilli (green arrowheads) even in a $Cad99C^{21\text{-}5/21\text{-}6}$ (E) or $Cad99C^{21\text{-}8/21\text{-}6}$ (F and G) mutant background. (H) Structure of transgenic Cad99C-Fl and Cad99CΔcyt::GFP proteins. Confocal images are shown in A–G, and accompanying Nomarski images are shown in panels marked with ′ or ″. Yellow arrows mark clone boundaries in A–D. Bars, 10 μm.

flects the close association between those movements and eggshell secretion.

Cad99C has an evolutionarily conserved function in microvillus biogenesis

Cad99C specifically localizes to the plasma membrane of microvilli and is distributed throughout their entire length. PCDH15 shows a similar subcellular distribution in stereocilia on the surface of hair cells in the cochlea (Ahmed et al., 2003a). In *PCDH15* mutant mice (*Ames waltzer*) and zebrafish (*orbiter*), stereocilia are splayed and their arrangement is severely disturbed, causing deafness (Alagramam et al., 2000, 2001; Raphael et al., 2001; Seiler et al., 2005). The function of PCDH15 in stereocilia, however, has remained unclear. Our study indicates that its *D. melanogaster* orthologue Cad99C is a potent regulator of microvillus size. Interestingly, PCDH15 is found at a higher concentration in the longer stereocilia of a staircase-like bundle of hair cell stereocilia (Ahmed et al., 2003a), and an irregular shortening of stereocilia in *Ames waltzer* mice was described previously (Alagramam et al., 2000; Raphael et al., 2001). This raises the possibility that PCDH15 regulates the length of stereocilia similar to Cad99C. In addition to being required for size regulation, Cad99C is also important for the normal shape and arrangement of microvilli. It will be interesting to determine in future studies whether the effect on size and on shape and arrangement of microvilli/stereocilia reflects two distinct functions of Cad99C/PCDH15 or whether they are two consequences of the same molecular function. Together, we propose that Cad99C/PCDH15-type cadherins have an evolutionarily conserved role in microvillus biogenesis.

During the course of evolution, Cad99C/PCDH15 cadherins have adapted to act in apparently very different apical actin-based protrusions, such as the follicle cell microvilli of fly ovaries and the complex stereocilia of the vertebrate cochlea.

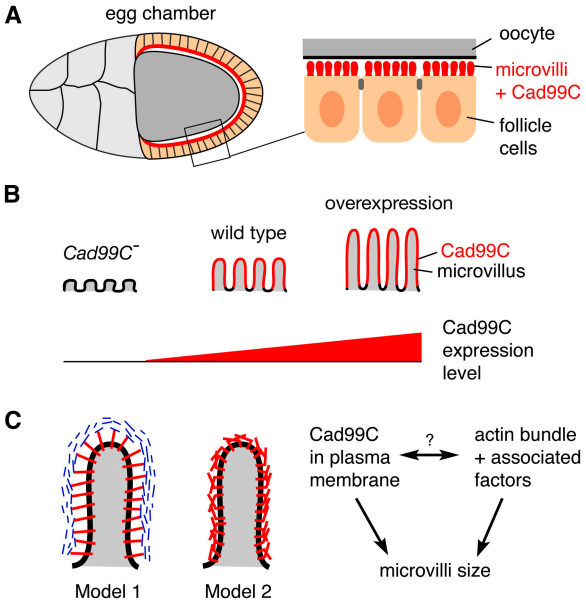

Figure 7. **Function of Cad99C: summary and model.** (A) Cad99C is located in apical microvilli of ovarian follicle cells. (B) The length of microvilli depends on the expression level of Cad99C. (C) Model 1 shows that the CDs of Cad99C (red) interact with an extracellular ligand (blue), which stabilizes the membrane or influences the dynamics of the actin bundle of the microvillus. Model 2 shows that the CDs of Cad99C assemble into a scaffold, stabilizing the microvillus membrane.

Moreover, loss of Cad99C causes subtle defects in eye rhabdomeres and mechanosensory bristles (unpublished data), indicating that Cad99C is also required for other actin-based protrusions. Similar to PCDH15, which is more widely expressed in epithelial tissues (Murcia and Woychik, 2001; Ahmed et al., 2003a), Cad99C is found on the apical surface of several ectodermal epithelia during *D. melanogaster* development, including the imaginal discs (Fig. S2, A–C, available at http://www.jcb.org/cgi/content/full/jcb.200507072/DC1; Schlichting et al., 2005). In wing imaginal discs as in the follicular epithelium, overexpression of Cad99C induces the formation of very large apical protrusions (Fig. S2, D and E). However, there are epithelial tissues that possess a microvillus brush border but do not express Cad99C at detectable levels, including the midgut (unpublished data). Cad99C is therefore not a general component of microvilli and may serve a biological function that is specifically required in a subset of microvilli. Alternatively, another member of the cadherin superfamily or other membrane protein might take the place of Cad99C in the microvilli of tissues that lack this cadherin.

A working model for Cad99C function

It is tempting to speculate that, as a cadherin, Cad99C may mediate homophilic adhesion between microvilli. However, follicle cell microvilli in wild type and after overexpression of Cad99C are clearly separated from each other, implying that Cad99C mediates neither homophilic nor heterophilic interactions between microvilli while promoting their outgrowth. This conclusion is corroborated by the behavior of cell clones that either lack or overexpress Cad99C. In imaginal discs where Cad99C is concentrated at the apical interface between cells, cell clones with reduced or increased levels of Cad99C expression have wiggly boundaries, indicating that they do not sort out from wild-type cells (Fig. S2 D; Schlichting et al., 2005; unpublished data). Furthermore, Cad99C located ectopically in the lateral membrane of follicle cells when overexpressed is not enriched at the border between Cad99C overexpressing cells compared with borders between wild-type and overexpressing cells (Fig. 6, B and D) as would be expected from a homophilic adhesion molecule. Similarly, in imaginal discs, the distribution of Cad99C along cell boundaries is uniform and independent of the concentration of Cad99C in neighboring cells (Fig. S2 D). Hence, our findings argue against a function of Cad99C in adhesion between adjacent plasma membranes.

A parallel bundle of actin filaments and associated factors that control their cross-linking and turnover are instrumental for the formation and stability of microvilli (for reviews see Bartles, 2000; DeRosier and Tilney, 2000; Lin et al., 2005). To what extent the plasma membrane of microvilli contributes to microvillus morphogenesis either by linking to the actin core or independent of it remains largely unexplored. PCDH15 appears to influence the actin cytoskeleton of stereocilia as the amount of F-actin in stereocilia of *PCDH15* mutant hair cells was reduced (Raphael et al., 2001). This effect is possibly mediated through its proposed interactions with the PDZ domain protein harmonin (Adato et al., 2005; Reiners et al., 2005). Among the USH1-associated proteins, harmonin has a central function, as it can also bind to CDH23, myosin VIIa, and SANS (Boëda et al., 2002; Siemens et al., 2002; Weil et al., 2003; Adato et al., 2005), and is able to interact with actin filaments promoting their bundling in cell culture (Boëda et al., 2002), thereby potentially linking cadherins on the cell surface to the actin cytoskeleton.

Unexpectedly, we found that a truncated form of Cad99C that lacks most of the cytoplasmic tail, including the putative PDZ domain–binding sites, causes the same excessive lengthening of microvilli as the full-length protein, even in a *Cad99C* mutant background. This shows that the PDZ domain–binding sites do not have an essential positive regulatory function in microvillus outgrowth. We cannot rule out that the remaining 31 juxtamembrane cytoplasmic amino acids interact with a cytoplasmic factor, but this short sequence contains no known motifs and is not conserved. Therefore, it seems likely that the membrane-bound extracellular domain of Cad99C is sufficient to promote microvillus extension independent of endogenous Cad99C. How does the extracellular domain of Cad99C control microvillus size? Our data are consistent with two attractive models for Cad99C activity (Fig. 7 C). The CDs of Cad99C could influence the microvillus actin core by binding to an extracellular ligand, which directly or indirectly connects to the actin bundle promoting polymerization. Alternatively, the Cad99C extracellular domain might stabilize the plasma membrane of a microvillus. This may be important because to lengthen a cellular protrusion, the force created by actin polymerization has to overcome the counteracting force caused by tension in the plasma membrane envelope while it is pushed outward (for review see Lin et al., 2005). Stabilization of the plasma membrane might alleviate the tension, allowing actin polymerization to proceed. The CDs of Cad99C could stabilize the plasma membrane either by binding to the extracellular matrix or by self-assembling into an extracellular meshwork that forms a supporting scaffold surrounding the microvillus. The striking conservation of the Cad99C/PCDH15 extracellular domains may reflect the geometric constraints imposed by such a scaffold. The latter model in particular would be consistent with the concentration dependency of Cad99C activity and with its effect on the size and shape of microvilli.

Materials and methods

Mutagenesis and fly strains

Deletion mutations of *Cad99C* (*CG31009*) were generated by excision of *P* element insertions *GE21053* and *GE23478* (GenExel, Inc.). 700 and 400 independent excision lines were established for *GE21034* and *GE23478*, respectively, and screened for lethality, morphological abnormalities, and sterility. Genomic deletions adjacent to the *P* element insertion points were found in all sterile but not in any of the tested fertile or lethal lines. Deletion breakpoints, which are based on the genomic clone AC007893 (Berkeley *Drosophila* Genome Project), were identified via PCR (Fig. 2 A) and sequencing using genomic DNA of homozygous mutant flies. Mutations $Cad99C^{21\text{-}5}$ (deletion breakpoints 70285 and 80821), $Cad99C^{21\text{-}8}$ (69477 and 77432), $Cad99C^{21\text{-}6}$ (70587 and 71521), $Cad99C^{21\text{-}9}$, and $Cad99C^{21\text{-}1}$ (70587 and 71335) were generated by excision of *GE21034*, and alleles $Cad99C^{23\text{-}4}$ (70653 and 71561), $Cad99C^{23\text{-}7}$ (70418 and 72926), and $Cad99C^{23\text{-}2}$ were produced via excision of *GE23478*. All phenotypic studies were conducted with two or more *Cad99C* alleles, which were derived from *GE21034*.

UAS expression lines used were *UAS-Cad99C-RNAi* (6-5D, chromosome X), *UAS-Cad99C-FL* (T2 and T5, chromosome X), *UAS-*

Cad99CΔcyt::GFP (18–10, chromosome X; for details see next paragraph), and *UAS-CD8::GFP* (Lee and Luo, 1999). Gal4 driver lines used were *da-Gal4* (P[*GAL4-da.G32*]UH1; Wodarz et al., 1995) and *Act5c>CD2>Gal4* (Pignoni et al., 1997). To induce expression of *UAS-Cad99C-FL* and *UAS-Cad99CΔcyt::GFP* in a *Cad99C* mutant background, a third chromosome carrying both *Act5c>CD2>Gal4* and *Cad99C*$^{21\text{-}6}$ was generated by meiotic recombination. Expression of FLPase (P[*hsFLP*]1; Golic, 1991), which activates the *Act5c>CD2>Gal4* FLPout cassette to clonally express Gal4 that in turn drives expression of *UAS*-constructs (Pignoni et al., 1997), was induced by a heat shock at 37°C (air incubator). For phenotypic analysis, females were heat shocked once for 15 or 30 min and dissected 2 d later to get mosaic ovaries with wild-type and *UAS* transgene–expressing cells; for Western blot analysis, females were heat shocked for 2 × 2 h for 2 d and then dissected to get ovaries, in which most follicle cells expressed *UAS-Cad99C-RNAi*. Oregon R was used as wild type.

Cad99C transgenes

Cad99C-FL, a 5.6-kb *Cad99C* cDNA that consists of a partial 5′ UTR (125 bp) and full-length coding region (5,118 bp) and 3′ UTR (391 bp), was generated from three overlapping cDNAs: EST LD23053 (Stapleton et al., 2002), MM1, and MM2. MM1 and MM2 were generated by RT-PCR via primers GGCTCCACTAGCGTAGGC and CCCTCGTCGTTGTCAGTG and CATCTTGGTGGTGAACGAGG and GCTATTGGCTTCCATTGACTC, respectively, and confirmed by sequencing. To generate *Cad99CΔcyt::GFP*, a fragment of *Cad99C-Fl* lacking 1,166 bp at the 3′ end was subcloned into pEGFP-N2 (CLONTECH Laboratories, Inc.) to express a fusion protein, in which GFP replaces the COOH-terminal region of Cad99C, deleting 256 of the 287 amino acids of the Cad99C cytoplasmic domain. A *Cad99C-RNAi* transgene was generated that allows induced expression of dsRNA for the purpose of RNAi (for review see Lee and Carthew, 2003). 1.1 kb of *Cad99C* coding sequence (342–1,436 bp of EST LD23053) in reverse (3′–5′) orientation was attached to a 0.5-kb linker containing two *Cad99C* introns (amplified with primers CGTAGAGAAGTACAGTGCGG and GCAGCCGCTATAGATGAAC using genomic wild-type DNA as a template), which was followed by a 0.7-kb fragment of the 1.1-kb *Cad99C* coding sequence (747–1,436 bp of EST LD23053) in forward (5′–3′) orientation. Constructs *Cad99C-FL*, *Cad99CΔcyt::GFP*, and *Cad99C-RNAi* were subcloned into a transformation vector (pUAST; Brand and Perrimon, 1993) to generate transgenic flies following standard procedures.

Eggshell analysis

To determine oviposition rates, batches of 21 females (4–5 d old, well fed) were allowed to lay eggs on yeasted apple juice agar plates for periods of 17 h at 25°C. To test the resistance of eggs to water loss, eggs (0–2.5 h old) were collected and kept on apple juice agar plates at 24°C, and desiccated eggs were counted every 2 h. To test the tolerance of eggs to hypochlorite, batches of 50 eggs (noncollapsed, 0–4 h old) were incubated in 2.6% sodium hypochlorite in PBS. Permeability of eggshells to vital dyes was tested by incubating eggs (noncollapsed, 0–7 h old) in 1% trypan blue or neutral red in PBS for 1 h, after which they were mounted in PBS and viewed immediately. Histological preparations were done according to Tepass and Hartenstein (1994).

Cad99C antibodies and detection of proteins and RNA

To generate Cad99C antibodies, peptides corresponding to aa 1090–1303 (extracellular peptide) and 1498–1701 (cytoplasmic peptide) of Cad99C were expressed and extracted as GST-fusion proteins and used to immunize guinea pigs and rats, respectively. Specificity of antisera was confirmed by comparing wild-type and *Cad99C* mutant tissue samples in Western blot analysis and by immunostaining. For immunostaining, primary antibodies used were polyclonal guinea pig α-Cad99C (GP5 1: 3,000), rabbit α-GFP (1:100; CLONTECH Laboratories, Inc.), rabbit α-DPatj (1:250; Tanentzapf et al., 2000), rabbit α-Nudel (NNDL, 1:400; LeMosy et al., 1998), rat α-Yolkless (No. 156, 1:150; Schönbaum et al., 2000), monoclonal rat α-DE-cadherin (DEcad2, 1:50; Oda et al., 1994), and mouse α-Arm (N2-71A1, 1:100; Peifer et al., 1993). Secondary antibodies (1:400) were conjugated to Cy3, Cy5 (Jackson ImmunoResearch Laboratories), or Alexa-488 (Invitrogen). F-actin was visualized with Phalloidin-Rhodamine (1:20; Invitrogen). For Western blot analysis, proteins from wild-type and *Cad99C* mutant adult ovaries were separated on a 6% SDS-PAGE gel, blotted onto a 0.1-μm nitrocellulose membrane (Schleicher & Schuell) using a methanol-free transfer, and detected with guinea pig α-Cad99C (GP5 1:10.000) or rat α-Cad99C (R7 1:1.000), and mouse α-Arm (N2-71A1, 1:500; Peifer et al., 1993) primary antibodies, HRP-conjugated secondary antibodies (1:1,000; Jackson ImmunoResearch Laboratories), and the ECL visualization system (GE Healthcare). Broad-range protein standards (prestained [GIBCO BRL] and unstained [Bio-Rad Laboratories]) were used to determine the molecular weight of proteins. For tissue in situ hybridizations, cDNA LD23053 (Stapleton et al., 2002) was used to generate a digoxigenin-labeled (Roche) DNA probe for *Cad99C*.

Imaging

Fluorescent images from preparations mounted in Vectashield (Vector Laboratories) were generated with a scanning laser confocal microscope (LSM510; Carl Zeiss MicroImaging, Inc.) using 40×/1.4 and 100×/1.4 Plan-Apo objectives. Confocal images displayed in Figs. 4–6 were taken at 65–85% anterior–posterior egg chamber length. Histological images were generated with an Axioskop (100×/1.4 Plan-Apo objective; Carl Zeiss MicroImaging, Inc.), and images of eggs were generated with a Stemi SV11 (Carl Zeiss MicroImaging, Inc.), using a digital camera (AxioCam) and Axiovision 2.05 or 4.3 software (Carl Zeiss MicroImaging, Inc.). All imaging was done at RT. Figures were processed using Photoshop 7 and Illustrator 10 (Adobe Systems) and graphs were generated with Prism 4 (GraphPad Software).

Online supplemental material

Fig. S1 shows sequence alignment of the CDs of Cad99C and PCDH15 and consensus sites for binding of Ca^{2+}. Fig. S2 shows that Cad99C is located on the apical surface of the wing disc epithelium and induces long apical protrusions when overexpressed. Online supplemental material is available at http://www.jcb.org/cgi/content/full/jcb.200507072/DC1.

We thank R. Winklbauer for critical comments on the manuscript. We thank A. Mahowald, E. LeMosy, and the Developmental Studies Hybridoma Bank for antibodies and GenExel, Inc. and the Bloomington *Drosophila* Stock Center for fly strains. We thank Nadja Ghani, Wendy Lee, Milena Pellikka, and Henry Hong for technical help.

This work was funded by grants MOP-42528 and MOP-74510 from the Canadian Institute of Health Research (to D. Godt).

Submitted: 15 July 2005
Accepted: 29 September 2005

References

Adato, A., V. Michel, Y. Kikkawa, J. Reiners, K.N. Alagramam, D. Weil, H. Yonekawa, U. Wolfrum, A. El-Amraoui, and C. Petit. 2005. Interactions in the network of Usher syndrome type 1 proteins. *Hum. Mol. Genet.* 14:347–356.

Ahmed, Z.M., S. Riazuddin, J. Ahmad, S.L. Bernstein, Y. Guo, M.F. Sabar, P. Sieving, A.J. Griffith, T.B. Friedman, I.A. Belyantseva, and E.R. Wilcox. 2003a. PCDH15 is expressed in the neurosensory epithelium of the eye and ear and mutant alleles are responsible for both USH1F and DFNB23. *Hum. Mol. Genet.* 12:3215–3223.

Ahmed, Z.M., S. Riazuddin, and E.R. Wilcox. 2003b. The molecular genetics of Usher syndrome. *Clin. Genet.* 63:431–444.

Alagramam, K.N., J. Zahorsky-Reeves, C.G. Wright, K.S. Pawlowski, L.C. Erway, L. Stubbs, and R.P. Woychik. 2000. Neuroepithelial defects of the inner ear in a new allele of the mouse mutation Ames waltzer. *Hear. Res.* 148:181–191.

Alagramam, K.N., C.L. Murcia, H.Y. Kwon, K.S. Pawlowski, C.G. Wright, and R.P. Woychik. 2001. The mouse Ames waltzer hearing-loss mutant is caused by mutation of Pcdh15, a novel protocadherin gene. *Nat. Genet.* 27:99–102.

Bartles, J.R. 2000. Parallel actin bundles and their multiple actin-bundling proteins. *Curr. Opin. Cell Biol.* 12:72–78.

Belyantseva, I.A., E.T. Boger, and T.B. Friedman. 2003. Myosin XVa localizes to the tips of inner ear sensory cell stereocilia and is essential for staircase formation of the hair bundle. *Proc. Natl. Acad. Sci. USA.* 100:13958–13963.

Belyantseva, I.A., E.T. Boger, S. Naz, G.I. Frolenkov, J.R. Sellers, Z.M. Ahmed, A.J. Griffith, and T.B. Friedman. 2005. Myosin-XVa is required for tip localization of whirlin and differential elongation of hair-cell stereocilia. *Nat. Cell Biol.* 7:148–156.

Boëda, B., A. El-Amraoui, A. Bahloul, R. Goodyear, L. Daviet, S. Blanchard, I. Perfettini, K.R. Fath, S. Shorte, J. Reiners, et al. 2002. Myosin VIIa, harmonin and cadherin 23, three Usher I gene products that cooperate to shape the sensory hair cell bundle. *EMBO J.* 21:6689–6699.

Borisy, G.G., and T.M. Svitkina. 2000. Actin machinery: pushing the envelope. *Curr. Opin. Cell Biol.* 12:104–112.

Brand, A.H., and N. Perrimon. 1993. Targeted gene expression as a means of altering cell fates and generating dominant phenotypes. *Development.* 118:401–415.

Celniker, S.E., D.A. Wheeler, B. Kronmiller, J.W. Carlson, A. Halpern, S. Patel, M. Adams, M. Champe, S.P. Dugan, E. Frise, et al. 2002. Finishing a whole-genome shotgun: release 3 of the *Drosophila melanogaster* euchromatic genome sequence. *Genome Biol.* 3:Research0079.1–0079.14.

Croce, A., G. Cassata, A. Disanza, M.C. Gagliani, C. Tacchetti, M.G. Malabarba, M.F. Carlier, G. Scita, R. Baumeister, and P.P. Di Fiore. 2004. A novel actin barbed-end-capping activity in EPS-8 regulates apical morphogenesis in intestinal cells of *Caenorhabditis elegans*. *Nat. Cell Biol.* 6:1173–1179.

DeRosier, D.J., and L.G. Tilney. 2000. F-actin bundles are derivatives of microvilli: what does this tell us about how bundles might form? *J. Cell Biol.* 148:1–6.

Frolenkov, G.I., I.A. Belyantseva, T.B. Friedman, and A.J. Griffith. 2004. Genetic insights into the morphogenesis of inner ear hair cells. *Nat. Rev. Genet.* 5:489–498.

Gautreau, A., D. Louvard, and M. Arpin. 2000. Morphogenic effects of ezrin require a phosphorylation-induced transition from oligomers to monomers at the plasma membrane. *J. Cell Biol.* 150:193–203.

Golic, K.G. 1991. Site-specific recombination between homologous chromosomes in *Drosophila*. *Science.* 252:958–961.

Grevengoed, E.E., D.T. Fox, J. Gates, and M. Peifer. 2003. Balancing different types of actin polymerization at distinct sites: roles for Abelson kinase and Enabled. *J. Cell Biol.* 163:1267–1279.

Hill, E., I.D. Broadbent, C. Chothia, and J. Pettitt. 2001. Cadherin superfamily proteins in *Caenorhabditis elegans* and *Drosophila melanogaster*. *J. Mol. Biol.* 305:1011–1024.

Horne-Badovinac, S., and D. Bilder. 2005. Mass transit: epithelial morphogenesis in the *Drosophila* egg chamber. *Dev. Dyn.* 232:559–574.

Karagiosis, S.A., and D.F. Ready. 2004. Moesin contributes an essential structural role in *Drosophila* photoreceptor morphogenesis. *Development.* 131:725–732.

Koch, A.W., K.L. Manzur, and W. Shan. 2004. Structure-based models of cadherin-mediated cell adhesion: the evolution continues. *Cell. Mol. Life Sci.* 61:1884–1895.

Lee, T., and L. Luo. 1999. Mosaic analysis with a repressible cell marker for studies of gene function in neuronal morphogenesis. *Neuron.* 22:451–461.

Lee, Y.S., and R.W. Carthew. 2003. Making a better RNAi vector for *Drosophila*: use of intron spacers. *Methods.* 30:322–329.

LeMosy, E.K., and C. Hashimoto. 2000. The nudel protease of *Drosophila* is required for eggshell biogenesis in addition to embryonic patterning. *Dev. Biol.* 217:352–361.

LeMosy, E.K., D. Kemler, and C. Hashimoto. 1998. Role of Nudel protease activation in triggering dorsoventral polarization of the *Drosophila* embryo. *Development.* 125:4045–4053.

Limbourg, B., and M. Zalokar. 1973. Permeabilization of *Drosophila* eggs. *Dev. Biol.* 35:382–387.

Lin, H.W., M.E. Schneider, and B. Kachar. 2005. When size matters: the dynamic regulation of stereocilia lengths. *Curr. Opin. Cell Biol.* 17:55–61.

Loomis, P.A., L. Zheng, G. Sekerkova, B. Changyaleket, E. Mugnaini, and J.R. Bartles. 2003. Espin cross-links cause the elongation of microvillus-type parallel actin bundles in vivo. *J. Cell Biol.* 163:1045–1055.

Mahowald, A.P. 1972. Ultrastructural observations on oogenesis in *Drosophila*. *J. Morphol.* 137:29–48.

Mahowald, A.P., and M.P. Kambysellis. 1980. Oogenesis. *In* The Genetics and Biology of *Drosophila*. Vol. 2. M. Ashburner and T.R.F. Wright, editors. Academic Press, New York. 141–224.

Mburu, P., M. Mustapha, A. Varela, D. Weil, A. El-Amraoui, R.H. Holme, A. Rump, R.E. Hardisty, S. Blanchard, R.S. Coimbra, et al. 2003. Defects in whirlin, a PDZ domain molecule involved in stereocilia elongation, cause deafness in the whirler mouse and families with DFNB31. *Nat. Genet.* 34:421–428.

Michel, V., R.J. Goodyear, D. Weil, W. Marcotti, I. Perfettini, U. Wolfrum, C.J. Kros, G.P. Richardson, and C. Petit. 2005. Cadherin 23 is a component of the transient lateral links in the developing hair bundles of cochlear sensory cells. *Dev. Biol.* 280:281–294.

Müller, U., and A. Littlewood-Evans. 2001. Mechanisms that regulate mechanosensory hair cell differentiation. *Trends Cell Biol.* 11:334–342.

Murcia, C.L., and R.P. Woychik. 2001. Expression of Pcdh15 in the inner ear, nervous system and various epithelia of the developing embryo. *Mech. Dev.* 105:163–166.

Oda, H., T. Uemura, Y. Harada, Y. Iwai, and M. Takeichi. 1994. A *Drosophila* homolog of cadherin associated with armadillo and essential for embryonic cell-cell adhesion. *Dev. Biol.* 165:716–726.

Patel, S.D., C.P. Chen, F. Bahna, B. Honig, and L. Shapiro. 2003. Cadherin-mediated cell-cell adhesion: sticking together as a family. *Curr. Opin. Struct. Biol.* 13:690–698.

Peifer, M., S. Orsulic, D. Sweeton, and E. Wieschaus. 1993. A role for the *Drosophila* segment polarity gene armadillo in cell adhesion and cytoskeletal integrity during oogenesis. *Development.* 118:1191–1207.

Petit, C. 2001. Usher syndrome: from genetics to pathogenesis. *Annu. Rev. Genomics Hum. Genet.* 2:271–297.

Pignoni, F., B. Hu, K.H. Zavitz, J. Xiao, P.A. Garrity, and S.L. Zipursky. 1997. The eye-specification proteins So and Eya form a complex and regulate multiple steps in *Drosophila* eye development. *Cell.* 91:881–891.

Raphael, Y., K.N. Kobayashi, G.A. Dootz, L.A. Beyer, D.F. Dolan, and M. Burmeister. 2001. Severe vestibular and auditory impairment in three alleles of Ames waltzer (av) mice. *Hear. Res.* 151:237–249.

Reiners, J., B. Reidel, A. El-Amraoui, B. Boeda, I. Huber, J. Reiners, T. Marker, K. Jurgens, B. Reidel, and U. Wolfrum. 2005. Photoreceptor expression of the Usher syndrome type 1 protein protocadherin 15 (USH1F) and its interaction with the scaffold protein harmonin (USH1C). *Mol. Vis.* 11:347–355.

Rzadzinska, A.K., M.E. Schneider, C. Davies, G.P. Riordan, and B. Kachar. 2004. An actin molecular treadmill and myosins maintain stereocilia functional architecture and self-renewal. *J. Cell Biol.* 164:887–897.

Saotome, I., M. Curto, and A.I. McClatchey. 2004. Ezrin is essential for epithelial organization and villus morphogenesis in the developing intestine. *Dev. Cell.* 6:855–864.

Schlichting, K., F. Demontis, and C. Dahmann. 2005. Cadherin Cad99C is regulated by Hedgehog signaling in *Drosophila*. *Dev. Biol.* 279:142–154.

Schönbaum, C.P., J.J. Perrino, and A.P. Mahowald. 2000. Regulation of the vitellogenin receptor during *Drosophila melanogaster* oogenesis. *Mol. Biol. Cell.* 11:511–521.

Seiler, C., K.C. Finger-Baier, O. Rinner, Y.V. Makhankov, H. Schwarz, S.C. Neuhauss, and T. Nicolson. 2005. Duplicated genes with split functions: independent roles of protocadherin15 orthologues in zebrafish hearing and vision. *Development.* 132:615–623.

Sekerkova, G., L. Zheng, P.A. Loomis, B. Changyaleket, D.S. Whitlon, E. Mugnaini, and J.R. Bartles. 2004. Espins are multifunctional actin cytoskeletal regulatory proteins in the microvilli of chemosensory and mechanosensory cells. *J. Neurosci.* 24:5445–5456.

Sheng, M., and C. Sala. 2001. PDZ domains and the organization of supramolecular complexes. *Annu. Rev. Neurosci.* 24:1–29.

Siemens, J., P. Kazmierczak, A. Reynolds, M. Sticker, A. Littlewood-Evans, and U. Muller. 2002. The Usher syndrome proteins cadherin 23 and harmonin form a complex by means of PDZ-domain interactions. *Proc. Natl. Acad. Sci. USA.* 99:14946–14951.

Siemens, J., C. Lillo, R.A. Dumont, A. Reynolds, D.S. Williams, P.G. Gillespie, and U. Müller. 2004. Cadherin 23 is a component of the tip link in hair-cell stereocilia. *Nature.* 428:950–955.

Söllner, C., G.J. Rauch, J. Siemens, R. Geisler, S.C. Schuster, U. Muller, and T. Nicolson. 2004. Mutations in cadherin 23 affect tip links in zebrafish sensory hair cells. *Nature.* 428:955–959.

Spradling, A.C. 1993. Developmental genetics of oogenesis. *In* The Development of *Drosophila melanogaster*. M. Bate and A. Martinez-Arias, editors. Cold Spring Harbor Laboratory Press, Cold Spring Harbor, NY. 1–70.

Stapleton, M., G. Liao, P. Brokstein, L. Hong, P. Carninci, T. Shiraki, Y. Hayashizaki, M. Champe, J. Pacleb, K. Wan, et al. 2002. The *Drosophila* gene collection: identification of putative full-length cDNAs for 70% of *D. melanogaster* genes. *Genome Res.* 12:1294–1300.

Tanentzapf, G., C. Smith, J. McGlade, and U. Tepass. 2000. Apical, lateral, and basal polarization cues contribute to the development of the follicular epithelium during *Drosophila* oogenesis. *J. Cell Biol.* 151:891–904.

Tepass, U., and V. Hartenstein. 1994. The development of cellular junctions in the *Drosophila* embryo. *Dev. Biol.* 161:563–596.

Tepass, U., K. Truong, D. Godt, M. Ikura, and M. Peifer. 2000. Cadherins in embryonic and neural morphogenesis. *Nat. Rev. Mol. Cell Biol.* 1:91–100.

Weil, D., A. El-Amraoui, S. Masmoudi, M. Mustapha, Y. Kikkawa, S. Laine, S. Delmaghani, A. Adato, S. Nadifi, Z.B. Zina, et al. 2003. Usher syndrome type I G (USH1G) is caused by mutations in the gene encoding SANS, a protein that associates with the USH1C protein, harmonin. *Hum. Mol. Genet.* 12:463–471.

Wodarz, A., U. Hinz, M. Engelbert, and E. Knust. 1995. Expression of crumbs confers apical character on plasma membrane domains of ectodermal epithelia of *Drosophila*. *Cell.* 82:67–76.

Zheng, L., G. Sekerkova, K. Vranich, L.G. Tilney, E. Mugnaini, and J.R. Bartles. 2000. The deaf jerker mouse has a mutation in the gene encoding the espin actin-bundling proteins of hair cell stereocilia and lacks espins. *Cell.* 102:377–385.